Analytical Solution of Biot's Equations Based on Potential Functions Method

Abolfazl Hasani Baferani
Acoustics Research Laboratory,
Department of Mechanical Engineering,
Amirkabir University of Technology
(Tehran Polytechnic),
No. 424, Hafez Avenue,
Tehran 15914, Iran
e-mail: a_hasani_baferani@aut.ac.ir

Abdolreza Ohadi
Associate Professor
Acoustics Research Laboratory,
Department of Mechanical Engineering,
Amirkabir University of Technology
(Tehran Polytechnic),
No. 424, Hafez Avenue,
Tehran 15914, Iran
e-mail: a_r_ohadi@aut.ac.ir

In this paper, a new analytical solution for Biot's equations is presented based on potential functions method. The primary coupled Biot's equations have been considered based on fluid and solid displacements in three-dimensional (3D) space. By defining some potential functions, the governing equations have been improved to a simpler form. Then the coupled Biot's equations have been replaced with four-decoupled equations, by doing some mathematical manipulations. For a case study, it is assumed that the incident wave is in xy-plane and for specific boundary conditions; the partial differential equations are converted to ordinary differential equations and solved analytically. Then two foams with different properties have been considered, and acoustical properties of these foams due to the new developed method have been compared with the corresponding results presented by transfer-matrix method. Good agreement between results verifies the new presented solution. Based on the potential function method, not only the acoustical properties of porous materials are calculated, but also the analytical values of all basic field variables, such as pressure, fluid, and solid displacements, are obtained for all points in the porous media. Furthermore, fundamental features, such as damped and undamped natural frequencies, and damping coefficient of porous materials are calculated by considering presented results. The obtained results show that maximum values of field variables, such as pressure, fluid, and solid displacements, happen at the damped natural frequencies of the porous media, as expected. By increasing material thickness, the effect of damping of porous material on damped natural frequency decreases. Damping decreases the first natural frequency of the foam up to 8.5%.
[DOI: 10.1115/1.4030715]

1 Introduction

Porous materials, composed of solid and fluid phases, play an important role in many branches of engineering science, e.g., acoustical engineering, petroleum industry, polymer and soil engineering, and biomechanics. Among of applications of porous material in acoustic field is the sound absorber. With increasing noise pollution in urban and industrial environments, application and designing of sound absorbing materials have become more important. Sound absorbers usually consist of porous materials such as polyurethane foam, and modeling and studying of these materials are important for designers. Undoubted, modeling of porous materials can be effective in advancing the science and help researchers studying different behavior of these materials.

By modeling of porous materials in sound absorbers not only the sound absorption coefficient of the material can be calculated, but also the variations of pressure, fluid, and solid displacements are established. The latter information can be very useful in the design of functionally graded porous material and microperforated panel absorbers. In addition, the variation of pressure and displacements provides useful suitable information in other applications of porous materials such as the extraction of oil from soil and research of bone in medical science.

Several models have been already proposed to study the behavior of porous materials [1,2]. These models can be divided into three categories included with assuming rigid solid, elastic solid, and experimental models. Among the proposed models assuming the solid phase to be elastic, the model presented by Biot is a more complete theoretical one [3,4], which has been expanded in medical applications in recent years. For example, Dai et al. [5] suggest that the Biot theory may provide a more robust and accurate model than other theories for wave propagation in the lungs over a wider frequency range. One of the most significant features presented in Biot's theory is the consideration of three types of waves in elastic porous material including two compression waves and one shear wave. Two different representations of Biot's equations have been presented by Atalla et al. [6] and Dazel et al. [7]. In 1988, Atalla et al. [6] presented the mixed (u_s,P) formulation for poroelastic materials. Based on this formulation, without addition of any assumption in Biot's equations, calculation time in finite-element method has been decreased. Also, Dazel et al. [7] proposed a new displacement formulation of Biot's linear equations based on solid and total displacement components. During the two past decades, researchers have presented different analytical and numerical mathematical methods for solving Biot's equation in all representations, some of them have been mentioned below.

Burridge and Vargas [8] presented the tensor Green's function of Biot's equations for a uniform space and used Laplace transform for solving governing equations. Moore and Lyons [9] derived a method from the Biot's theory for evaluating sound absorption characteristics by using an impedance matrix. They presented the variation of real and imaginary part of impedance through thickness and discussed about them. Chin et al. [10] considered matrix equations and presented acoustic characteristics for pulse propagation at normal incidence through a fluid-saturated porous medium. Allard et al. [11,12] proposed the transfer-matrix method for solving Biot's equations both for normal and oblique incident waves. To the best of author's knowledge, the results presented in different papers by transfer-matrix method are limited to surface impedance and absorption coefficients for porous materials. Bolton et al. [13] presented analytical method for solving Biot's equations. They considered isotropic porous materials and expressed solid and fluid displacement components as the sum of

Contributed by the Noise Control and Acoustics Division of ASME for publication in the Journal of Vibration and Acoustics. Manuscript received June 16, 2014; final manuscript received April 21, 2015; published online July 10, 2015. Assoc. Editor: Liang-Wu Cai.

irrotational and divergence-free components. Kang and Bolton [14] used finite element method for prediction of the acoustical behavior of foam-treated systems having finite dimensions. Also, Goransson [15,16] presented a fully symmetrical finite element solution for the coupled Biot's equations and investigated the acoustical behavior of porous materials. Tanneau et al. [17] used the boundary element method to solve coupled acoustical problems. Most of the above-mentioned solutions have some restrictions such as the mathematical complexity, numerical approximations, and limitations in the calculation of field variables.

In this paper, a new analytical method for solving Biot's equations is presented by using potential functions. In this technique, by defining some potential functions, Biot's equations are converted to a simpler form. Consequently, the six-coupled Biot's equations are changed to four-decoupled equations, by doing some mathematical manipulations. It is assumed that the incident wave is in *xy*-plane, so the partial differential equations change to ordinary differential equations. The six unknown parameters of the solution of differential equations are obtained by applying the boundary conditions. With this method, any number of layers with different compositions of porous material can be studied. One of the advantages of the potential function method compared to other methods is its simple mathematical calculation. In addition, the ability of potential function method to calculate different mechanical and acoustical filed variables of porous material, i.e., pressure, solid, and fluid displacements, represents the strength of this method.

Section 2 of this paper proposes the decoupling of Biot's equations in 3D space. In this section, the six-coupled Biot's equations are converted to four-decoupled equations. To simplify the expressions for the field variables, it is assumed in Sec. 3 that the system is excited by incident plane waves and the porous material has finite thickness and infinite lateral dimensions. The boundary conditions are applied in Sec. 4 to obtain the unknown parameters of solution. Section 5 presented calculation method of absorption coefficient, and Sec. 6 proposes the verification of the new solution method with the corresponding results of the transfer-matrix method. Some advantages of the potential function method are presented by comparison with other methods in Sec. 7. Finally, results and discussion are given in Secs. 8 and 9.

2 Decoupling of Biot's Equations Via Potential Function Method

The primary Biot's equations written in terms of solid and fluid displacements have been presented as [3,4]

$$\begin{aligned}(P-N)\ \mathrm{grad}(\mathrm{div}\boldsymbol{u}_s)+Q\quad \mathrm{grad}(\mathrm{div}\boldsymbol{u}_f)+N\\ \nabla^2\boldsymbol{u}_s=\tilde{\rho}_{11}\ddot{\boldsymbol{u}}_s+\tilde{\rho}_{12}\ddot{\boldsymbol{u}}_f\end{aligned}\tag{1}$$

$$R\ \mathrm{grad}(\mathrm{div}\boldsymbol{u}_f)+Q\ \mathrm{grad}(\mathrm{div}\boldsymbol{u}_s)=\tilde{\rho}_{12}\ddot{\boldsymbol{u}}_s+\tilde{\rho}_{22}\ddot{\boldsymbol{u}}_f\tag{2}$$

where $\boldsymbol{u}_s$ and $\boldsymbol{u}_f$ are solid and fluid displacement components, respectively. In addition, the superscript dot denotes partial differentials with respect to time $(\dot{(\,)}=\partial(\,)/\partial t)$. The coefficients $\tilde{\rho}_{11},\tilde{\rho}_{12}$, and $\tilde{\rho}_{22}$ are effective mass densities, P, Q, and R represent the elastic coefficients of the porous medium presented by Biot and Willis [18], and N is the shear modulus. The effective densities are given by

$$\begin{aligned}\tilde{\rho}_{11}&=(1-\phi)\rho_s-\tilde{\rho}_{12}\\ \tilde{\rho}_{22}&=\phi\rho_f-\tilde{\rho}_{12}\\ \tilde{\rho}_{12}&=(1-\alpha'_\infty)\phi\rho_f\end{aligned}\tag{3}$$

where ρ_s and ρ_f are the mass densities of the skeleton and fluid, respectively. Also parameters ϕ and α'_∞ represent porosity and dynamic tortuosity, respectively. In addition, the elastic coefficients are defined as

$$\begin{aligned}P&=\frac{(1-\phi)\left[1-\phi-\frac{K_b}{K_s}\right]K_s+\phi\frac{K_s}{K_f}K_b}{1-\phi-\frac{K_b}{K_s}+\phi\frac{K_s}{K_f}}+\frac{4}{3}N\\ Q&=\frac{\left[1-\phi-\frac{K_b}{K_s}\right]\phi K_s}{1-\phi-\frac{K_b}{K_s}+\phi\frac{K_s}{K_f}}\\ R&=\frac{\phi^2K_s}{1-\phi-\frac{K_b}{K_s}+\phi\frac{K_s}{K_f}}\end{aligned}\tag{4}$$

where K_s is the bulk modulus of the elastic solid, K_b denotes the bulk modulus of the frame in vacuum, and K_f is the bulk modulus of the fluid. It is mentioned that the dynamic tortuosity considered in this article is based on the model of Johnson et al. [19], and the bulk modulus of the fluid is based on Champoux–Allard model [20]. In addition, the compressible model is considered in this study but for the sake of example, it is assumed that $K_s \gg K_f$ because the elastic modulus of the solid part is not available. Furthermore, tortuosity and bulk modulus can be represented by other models (i.e., Lafrage or Pride models) as can be found in Ref. [21].

By considering time dependency as $e^{j\omega t}$, for the solid and fluid displacements, Eqs. (1) and (2) can be expanded as

$$P\frac{\partial}{\partial x}\left[\frac{\partial u_s^1}{\partial x}+\frac{\partial u_s^2}{\partial y}+\frac{\partial u_s^3}{\partial z}\right]+N\left(\frac{\partial}{\partial y}\left[\frac{\partial u_s^1}{\partial y}-\frac{\partial u_s^2}{\partial x}\right]+\frac{\partial}{\partial z}\left[\frac{\partial u_s^1}{\partial z}-\frac{\partial u_s^3}{\partial x}\right]\right)+Q\frac{\partial}{\partial x}\left[\frac{\partial u_f^1}{\partial x}+\frac{\partial u_f^2}{\partial y}+\frac{\partial u_f^3}{\partial z}\right]=-\omega^2\tilde{\rho}_{11}u_s^1-\omega^2\tilde{\rho}_{12}u_f^1\tag{5}$$

$$P\frac{\partial}{\partial y}\left[\frac{\partial u_s^1}{\partial x}+\frac{\partial u_s^2}{\partial y}+\frac{\partial u_s^3}{\partial z}\right]-N\left(\frac{\partial}{\partial x}\left[\frac{\partial u_s^1}{\partial y}-\frac{\partial u_s^2}{\partial x}\right]+\frac{\partial}{\partial z}\left[\frac{\partial u_s^3}{\partial y}-\frac{\partial u_s^2}{\partial z}\right]\right)+Q\frac{\partial}{\partial y}\left[\frac{\partial u_f^1}{\partial x}+\frac{\partial u_f^2}{\partial y}+\frac{\partial u_f^3}{\partial z}\right]=-\omega^2\tilde{\rho}_{11}u_s^2-\omega^2\tilde{\rho}_{12}u_f^2\tag{6}$$

$$P\frac{\partial}{\partial z}\left[\frac{\partial u_s^1}{\partial x}+\frac{\partial u_s^2}{\partial y}+\frac{\partial u_s^3}{\partial z}\right]+N\left(\frac{\partial}{\partial x}\left[\frac{\partial u_s^3}{\partial x}-\frac{\partial u_s^1}{\partial z}\right]+\frac{\partial}{\partial y}\left[\frac{\partial u_s^3}{\partial y}-\frac{\partial u_s^2}{\partial z}\right]\right)+Q\frac{\partial}{\partial z}\left[\frac{\partial u_f^1}{\partial x}+\frac{\partial u_f^2}{\partial y}+\frac{\partial u_f^3}{\partial z}\right]=-\omega^2\tilde{\rho}_{11}u_s^3-\omega^2\tilde{\rho}_{12}u_f^3\tag{7}$$

$$R\frac{\partial}{\partial x}\left[\frac{\partial u_f^1}{\partial x}+\frac{\partial u_f^2}{\partial y}+\frac{\partial u_f^3}{\partial z}\right]+Q\frac{\partial}{\partial x}\left[\frac{\partial u_s^1}{\partial x}+\frac{\partial u_s^2}{\partial y}+\frac{\partial u_s^3}{\partial z}\right]=-\omega^2\tilde{\rho}_{12}u_s^1-\omega^2\tilde{\rho}_{22}u_f^1 \tag{8}$$

$$R\frac{\partial}{\partial y}\left[\frac{\partial u_f^1}{\partial x}+\frac{\partial u_f^2}{\partial y}+\frac{\partial u_f^3}{\partial z}\right]+Q\frac{\partial}{\partial y}\left[\frac{\partial u_s^1}{\partial x}+\frac{\partial u_s^2}{\partial y}+\frac{\partial u_s^3}{\partial z}\right]=-\omega^2\tilde{\rho}_{12}u_s^2-\omega^2\tilde{\rho}_{22}u_f^2 \tag{9}$$

$$R\frac{\partial}{\partial z}\left[\frac{\partial u_f^1}{\partial x}+\frac{\partial u_f^2}{\partial y}+\frac{\partial u_f^3}{\partial z}\right]+Q\frac{\partial}{\partial z}\left[\frac{\partial u_s^1}{\partial x}+\frac{\partial u_s^2}{\partial y}+\frac{\partial u_s^3}{\partial z}\right]=-\omega^2\tilde{\rho}_{12}u_s^3-\omega^2\tilde{\rho}_{22}u_f^3 \tag{10}$$

where u_s^1, u_s^2, and u_s^3 are components of solid displacement in x, y, and z direction, respectively. Also u_f^1, u_f^2, and u_f^3 denote components of fluid displacement in different directions. Equations (5)–(10) can be rewritten as

$$P\frac{\partial\phi_1}{\partial x}+N\left(\frac{\partial\phi_2}{\partial y}+\frac{\partial\phi_3}{\partial z}\right)+Q\frac{\partial\phi_5}{\partial x}+\omega^2\tilde{\rho}_{11}u_s^1+\omega^2\tilde{\rho}_{12}u_f^1=0 \tag{11}$$

$$P\frac{\partial\phi_1}{\partial y}-N\left(\frac{\partial\phi_2}{\partial x}+\frac{\partial\phi_4}{\partial z}\right)+Q\frac{\partial\phi_5}{\partial y}+\omega^2\tilde{\rho}_{11}u_s^2+\omega^2\tilde{\rho}_{12}u_f^2=0 \tag{12}$$

$$P\frac{\partial\phi_1}{\partial z}+N\left(\frac{\partial\phi_4}{\partial y}-\frac{\partial\phi_3}{\partial x}\right)+Q\frac{\partial\phi_5}{\partial z}+\omega^2\tilde{\rho}_{11}u_s^3+\omega^2\tilde{\rho}_{12}u_f^3=0 \tag{13}$$

$$R\frac{\partial\phi_5}{\partial x}+Q\frac{\partial\phi_1}{\partial x}+\omega^2\tilde{\rho}_{12}u_s^1+\omega^2\tilde{\rho}_{22}u_f^1=0 \tag{14}$$

$$R\frac{\partial\phi_5}{\partial y}+Q\frac{\partial\phi_1}{\partial y}+\omega^2\tilde{\rho}_{12}u_s^2+\omega^2\tilde{\rho}_{22}u_f^2=0 \tag{15}$$

$$R\frac{\partial\phi_5}{\partial z}+Q\frac{\partial\phi_1}{\partial z}+\omega^2\tilde{\rho}_{12}u_s^3+\omega^2\tilde{\rho}_{22}u_f^3=0 \tag{16}$$

The parameters $\phi_i (i=1,2,\ldots,5)$ are defined as

$$\begin{aligned}\phi_1&=\frac{\partial u_s^1}{\partial x}+\frac{\partial u_s^2}{\partial y}+\frac{\partial u_s^3}{\partial z}\\ \phi_2&=\frac{\partial u_s^1}{\partial y}-\frac{\partial u_s^2}{\partial x}\\ \phi_3&=\frac{\partial u_s^1}{\partial z}-\frac{\partial u_s^3}{\partial x}\\ \phi_4&=\frac{\partial u_s^3}{\partial y}-\frac{\partial u_s^2}{\partial z}\\ \phi_5&=\frac{\partial u_f^1}{\partial x}+\frac{\partial u_f^2}{\partial y}+\frac{\partial u_f^3}{\partial z}\end{aligned} \tag{17}$$

By differentiating Eqs. (11), (12), and (13) with respect to x, y, and z, respectively, the resulted equations are obtained as

$$P\frac{\partial^2\phi_1}{\partial x^2}+N\left(\frac{\partial^2\phi_2}{\partial y\partial x}+\frac{\partial^2\phi_3}{\partial z\partial x}\right)+Q\frac{\partial^2\phi_5}{\partial x^2}+\omega^2\tilde{\rho}_{11}\frac{\partial u_s^1}{\partial x}+\omega^2\tilde{\rho}_{12}\frac{\partial u_f^1}{\partial x}=0 \tag{18}$$

$$P\frac{\partial^2\phi_1}{\partial y^2}-N\left(\frac{\partial^2\phi_2}{\partial y\partial x}+\frac{\partial^2\phi_4}{\partial z\partial y}\right)+Q\frac{\partial^2\phi_5}{\partial y^2}+\omega^2\tilde{\rho}_{11}\frac{\partial u_s^2}{\partial y}+\omega^2\tilde{\rho}_{12}\frac{\partial u_f^2}{\partial y}=0 \tag{19}$$

$$P\frac{\partial^2\phi_1}{\partial z^2}+N\left(\frac{\partial^2\phi_4}{\partial y\partial z}-\frac{\partial^2\phi_3}{\partial x\partial z}\right)+Q\frac{\partial^2\phi_5}{\partial z^2}+\omega^2\tilde{\rho}_{11}\frac{\partial u_s^3}{\partial z}+\omega^2\tilde{\rho}_{12}\frac{\partial u_f^3}{\partial z}=0 \tag{20}$$

Summation of Eqs. (18)–(20) yields

$$P\nabla^2\phi_1+Q\nabla^2\phi_5+\omega^2\tilde{\rho}_{11}\phi_1+\omega^2\tilde{\rho}_{12}\phi_5=0 \tag{21}$$

where ∇^2 is Laplacian operator in Cartesian coordinates. Equations (11) and (12) are differentiated with respect to y and x, respectively. The summation of the obtained equations results in Eq. (22). The same procedure is applied both for Eqs. (12) and (13) with respect to z and y and for Eqs. (11) and (13) with respect to z and x, respectively. Equations (23) and (24) can be finally obtained as follows:

$$N\nabla^2\phi_2+\omega^2\tilde{\rho}_{11}\phi_2+\omega^2\tilde{\rho}_{12}\phi_6=0 \tag{22}$$

$$N\nabla^2\phi_4+\omega^2\tilde{\rho}_{11}\phi_4+\omega^2\tilde{\rho}_{12}\phi_7=0 \tag{23}$$

$$N\nabla^2\phi_3+\omega^2\tilde{\rho}_{11}\phi_3+\omega^2\tilde{\rho}_{12}\phi_8=0 \tag{24}$$

By doing the same above procedure for Eqs. (14)–(16) yields

$$\phi_6=-\frac{\tilde{\rho}_{12}}{\tilde{\rho}_{22}}\phi_2 \tag{25}$$

$$\phi_7=-\frac{\tilde{\rho}_{12}}{\tilde{\rho}_{22}}\phi_4 \tag{26}$$

$$\phi_8=-\frac{\tilde{\rho}_{12}}{\tilde{\rho}_{22}}\phi_3 \tag{27}$$

where the parameters ϕ_6 through ϕ_8 have been defined as

$$\phi_6=\frac{\partial u_f^1}{\partial y}-\frac{\partial u_f^2}{\partial x},\quad \phi_7=\frac{\partial u_f^3}{\partial y}-\frac{\partial u_f^2}{\partial z},\quad \phi_8=\frac{\partial u_f^1}{\partial z}-\frac{\partial u_f^3}{\partial x} \tag{28}$$

Substituting Eqs. (25)–(27) into Eqs. (22)–(24) yields

$$N\nabla^2\phi_2+\omega^2\left(\tilde{\rho}_{11}-\frac{\tilde{\rho}_{12}^2}{\tilde{\rho}_{22}}\right)\phi_2=0 \tag{29}$$

$$N\nabla^2\phi_4+\omega^2\left(\tilde{\rho}_{11}-\frac{\tilde{\rho}_{12}^2}{\tilde{\rho}_{22}}\right)\phi_4=0 \tag{30}$$

$$N\nabla^2\phi_3+\omega^2\left(\tilde{\rho}_{11}-\frac{\tilde{\rho}_{12}^2}{\tilde{\rho}_{22}}\right)\phi_3=0 \tag{31}$$

Therefore, parameters ϕ_2, ϕ_3, and ϕ_4 have been decoupled. By differentiating Eqs. (14)–(16) with respect to x, y, and z,

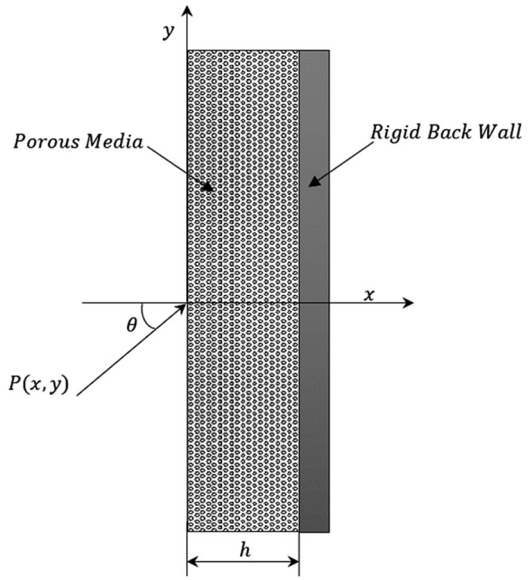

Fig. 1 Incident plane wave exciting porous media

Table 1 Properties of two different foams [21,22]

	Foam 1	Foam 2
Porosity ϕ	0.99	0.98
Flow resistivity $\sigma(\mathrm{Ns/m^4})$	10,900	6600
Tortuosity α_∞	1.02	1.03
Viscous characteristic length $\Lambda(\mu\mathrm{m})$	130	200
Thermal characteristic length $\Lambda'(\mu\mathrm{m})$	192	380
Mass density $\rho_1(\mathrm{kg/m^3})$	8.43	11.2
Young's modulus E (Pa)	195,000	293×10^6
Poisson's ratio ν	0.42	0.2
Structural loss factor η_s	0.05	0.06

respectively, and summation of the resulted equations, the following relation can be obtained:

$$Q\nabla^2\phi_1 + R\nabla^2\phi_5 + \omega^2\tilde{\rho}_{12}\phi_1 + \omega^2\tilde{\rho}_{22}\phi_5 = 0 \tag{32}$$

Now by considering Eqs. (21) and (32) and eliminating $\nabla^2\phi_5$ from these equations yield

$$\lambda_1\nabla^2\phi_1 + \lambda_2\phi_1 + \lambda_3\phi_5 = 0 \tag{33}$$

where

$$\lambda_1 = RP - Q^2, \quad \lambda_2 = \omega^2(R\tilde{\rho}_{11} - Q\tilde{\rho}_{12}),$$
$$\lambda_3 = \omega^2(R\tilde{\rho}_{12} - Q\tilde{\rho}_{22}) \tag{34}$$

The potential function ϕ_5 can be obtained from Eq. (33) as follows:

$$\phi_5 = -\frac{\lambda_1}{\lambda_3}\nabla^2\phi_1 - \frac{\lambda_2}{\lambda_3}\phi_1 \tag{35}$$

Substituting Eq. (35) into Eq. (21) yields

$$-\frac{Q\lambda_1}{\lambda_3}\nabla^4\phi_1 + \left[P - \frac{Q\lambda_2}{\lambda_3} - \frac{\omega^2\tilde{\rho}_{12}\lambda_1}{\lambda_3}\right]\nabla^2\phi_1 + \left[\omega^2\tilde{\rho}_{11} - \frac{\omega^2\tilde{\rho}_{12}\lambda_2}{\lambda_3}\right]\phi_1 = 0 \tag{36}$$

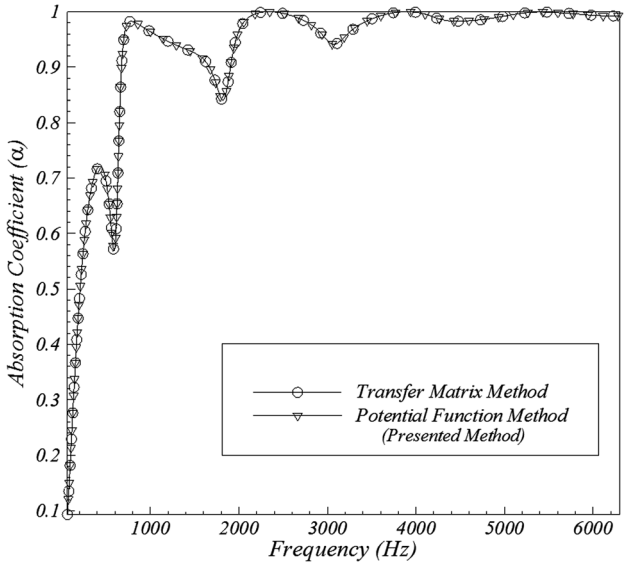

Fig. 2 Variation of absorption coefficient versus frequency for foam 1 ($h = 0.1$ m)—comparison between potential function and transfer-matrix methods

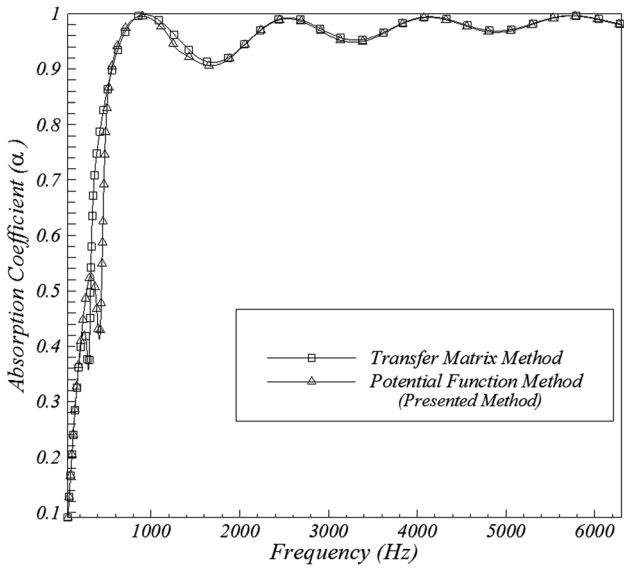

Fig. 3 Variation of absorption coefficient versus frequency for foam 2 ($h = 0.1$ m)—comparison between potential function and transfer-matrix methods

By considering four Eqs. (29)–(31) and (36), it can be seen that all potential functions have been decoupled. Other parameters ϕ_5 through ϕ_8 can be determined from parameters ϕ_1 through ϕ_4 using Eqs. (25)–(27) and (35).

By applying the incident waveform, decoupled equations can easily be analytically solved and each of the variables can be calculated for all points of the porous media. These solutions contain ten unknown parameters (C_1 through C_{10}), which can be obtained by applying all boundary conditions.

The field variables u_s^1 and u_f^1 can be obtained by considering Eqs. (11) and (14). In addition, the parameters u_s^2, u_f^2 and u_s^3, u_f^3 can be similarly acquired from Eqs. (12), (15), (13), and (16), respectively. Finally, we have

$$u_s^1 = \frac{\lambda_7}{\lambda_6}\frac{\partial\phi_1}{\partial x} + \frac{\lambda_8}{\lambda_6}\frac{\partial\phi_5}{\partial x} + \frac{N\tilde{\rho}_{22}}{\lambda_6}\left(\frac{\partial\phi_2}{\partial y} + \frac{\partial\phi_3}{\partial z}\right) \tag{37}$$

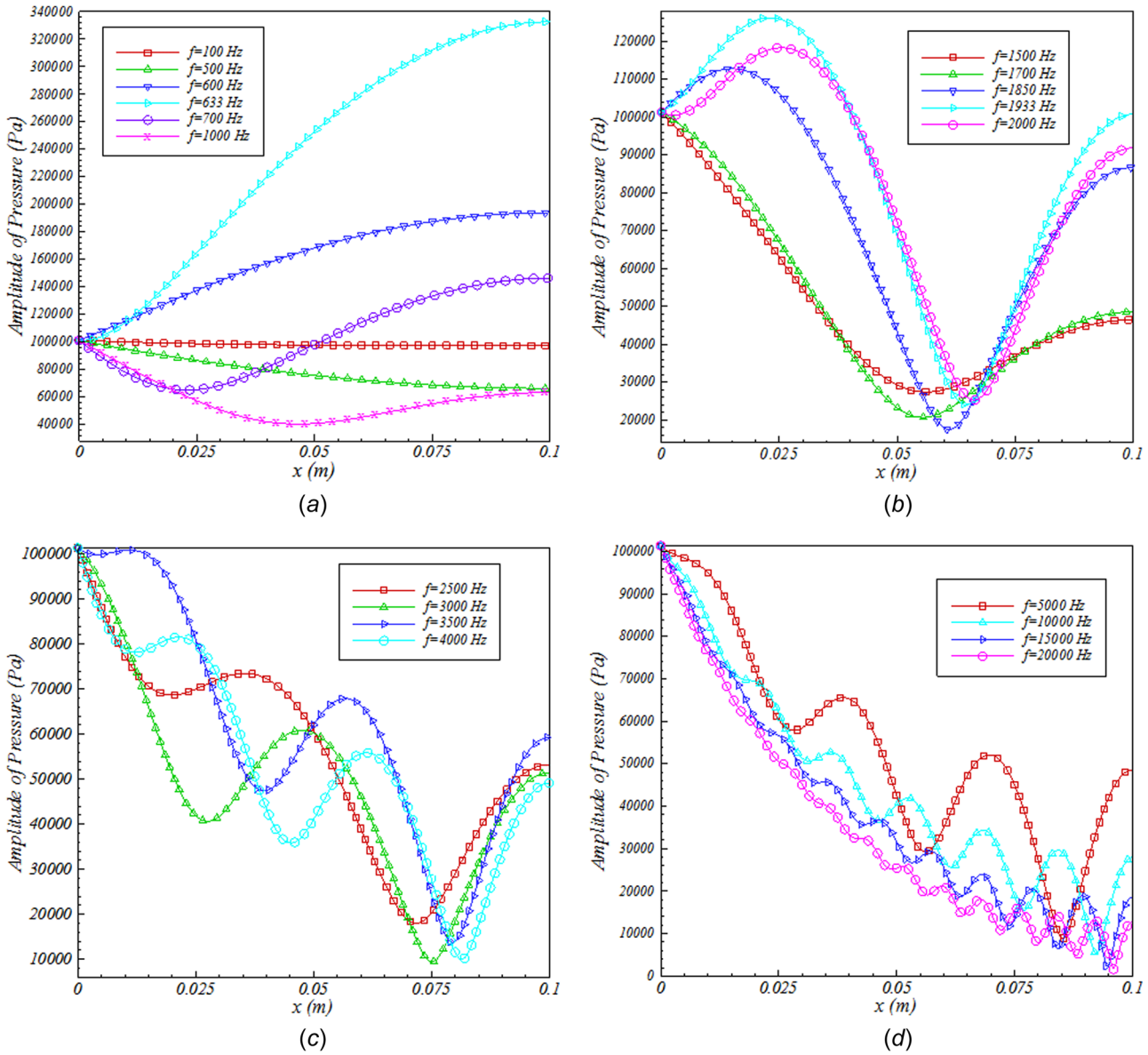

Fig. 4 Variation of amplitude of pressure in thickness direction for different frequencies in normal incident ($h = 0.1$m)

$$u_f^1 = -\frac{\lambda_4}{\lambda_6}\frac{\partial\phi_1}{\partial x} - \frac{\lambda_5}{\lambda_6}\frac{\partial\phi_5}{\partial x} - \frac{N\tilde{\rho}_{12}}{\lambda_6}\left(\frac{\partial\phi_2}{\partial y} + \frac{\partial\phi_3}{\partial z}\right) \tag{38}$$

$$u_s^2 = \frac{\lambda_7}{\lambda_6}\frac{\partial\phi_1}{\partial y} + \frac{\lambda_8}{\lambda_6}\frac{\partial\phi_5}{\partial y} - \frac{N\tilde{\rho}_{22}}{\lambda_6}\left(\frac{\partial\phi_2}{\partial x} + \frac{\partial\phi_4}{\partial z}\right) \tag{39}$$

$$u_f^2 = -\frac{\lambda_4}{\lambda_6}\frac{\partial\phi_1}{\partial y} - \frac{\lambda_5}{\lambda_6}\frac{\partial\phi_5}{\partial y} + \frac{N\tilde{\rho}_{12}}{\lambda_6}\left(\frac{\partial\phi_2}{\partial x} + \frac{\partial\phi_4}{\partial z}\right) \tag{40}$$

$$u_s^3 = \frac{\lambda_7}{\lambda_6}\frac{\partial\phi_1}{\partial z} + \frac{\lambda_8}{\lambda_6}\frac{\partial\phi_5}{\partial z} + \frac{N\tilde{\rho}_{22}}{\lambda_6}\left(\frac{\partial\phi_4}{\partial y} - \frac{\partial\phi_3}{\partial x}\right) \tag{41}$$

$$u_f^3 = -\frac{\lambda_4}{\lambda_6}\frac{\partial\phi_1}{\partial z} - \frac{\lambda_5}{\lambda_6}\frac{\partial\phi_5}{\partial z} + \frac{N\tilde{\rho}_{12}}{\lambda_6}\left(\frac{\partial\phi_4}{\partial y} - \frac{\partial\phi_3}{\partial x}\right) \tag{42}$$

Furthermore, pressure in porous media can be obtained as

$$p(x,y,z) = -\frac{K_f}{\phi}\left(\frac{\partial u_t^1}{\partial x} + \frac{\partial u_t^2}{\partial y} + \frac{\partial u_t^3}{\partial z}\right) \tag{43}$$

where $\boldsymbol{u}_t$ is the total displacement ($\boldsymbol{u}_t = \phi\boldsymbol{u}_f + (1-\phi)\boldsymbol{u}_s$). Total stress components applied to porous media can be presented as

$$\sigma_{11}^t = \left(K_b - \frac{2N}{3}\right)\left(\frac{\partial u_s^1}{\partial x} + \frac{\partial u_s^2}{\partial y} + \frac{\partial u_s^3}{\partial z}\right) - p(x,y,z) + 2N\frac{\partial u_s^1}{\partial x} \tag{44}$$

$$\sigma_{22}^t = \left(K_b - \frac{2N}{3}\right)\left(\frac{\partial u_s^1}{\partial x} + \frac{\partial u_s^2}{\partial y} + \frac{\partial u_s^3}{\partial z}\right) - p(x,y,z) + 2N\frac{\partial u_s^2}{\partial y} \tag{45}$$

$$\sigma_{33}^t = \left(K_b - \frac{2N}{3}\right)\left(\frac{\partial u_s^1}{\partial x} + \frac{\partial u_s^2}{\partial y} + \frac{\partial u_s^3}{\partial z}\right) - p(x,y,z) + 2N\frac{\partial u_s^3}{\partial z} \tag{46}$$

$$\sigma_{12}^t = N\left(\frac{\partial u_s^1}{\partial y} + \frac{\partial u_s^2}{\partial x}\right) \tag{47}$$

$$\sigma_{13}^t = N\left(\frac{\partial u_s^1}{\partial z} + \frac{\partial u_s^3}{\partial x}\right) \tag{48}$$

$$\sigma_{23}^t = N\left(\frac{\partial u_s^2}{\partial z} + \frac{\partial u_s^3}{\partial y}\right) \tag{49}$$

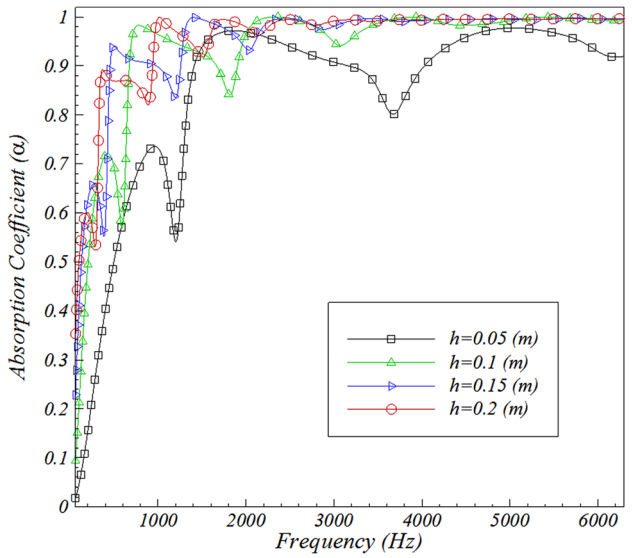

Fig. 5 Variation of absorption coefficient of foam 1 versus excitation frequency in the incident direction for four material thicknesses

Also, boundary conditions in porous media can be obtained based on Hamilton's principle. These boundary conditions yield in general form as

$$\begin{aligned}
&\delta u_s^1 = 0 \quad \text{or} \quad \sigma_{11}^t + \sigma_{12}^t + \sigma_{13}^t = \sigma_{\text{air}} \\
&\delta u_s^2 = 0 \quad \text{or} \quad \sigma_{21}^t + \sigma_{22}^t + \sigma_{23}^t = \sigma_{\text{air}} \\
&\delta u_s^3 = 0 \quad \text{or} \quad \sigma_{31}^t + \sigma_{32}^t + \sigma_{33}^t = \sigma_{\text{air}} \\
&\delta u_f^1 = 0 \quad \text{or} \quad \sigma_{11}^f = -\phi p^e \\
&\delta u_f^2 = 0 \quad \text{or} \quad \sigma_{22}^f = -\phi p^e \\
&\delta u_f^3 = 0 \quad \text{or} \quad \sigma_{33}^f = -\phi p^e
\end{aligned} \tag{50}$$

where σ_{air} is the stress of air applied to porous media. Also, $\sigma_{ii}^f (i = 1, 2, 3)$ are the fluid stress components and p^e indicate the pressure in the free air at contact surface with porous layer.

3 Wave Propagation in Porous Media

In this section, an incident plane wave excites the porous medium, and it is assumed that the porous material is in finite thickness and infinite lateral dimensions. The incident plane wave and the coordinate system of porous media are shown in Fig. 1. Based on this assumption, pressure of the incident wave is expected to be

$$p(x, y) = p(x) e^{-jky \sin\theta} \tag{51}$$

where $k = \omega/c_0$ is the acoustic wave number, ω is the circular frequency, and c_0 is the speed of sound in the surrounding acoustic medium. Also θ denotes the angle of incidence with respect to the x axis.

All variables can be written in the xy-plane, and these variables have the same exponential dependency. The solid and fluid displacements and potential functions are expressed as

$$\begin{aligned}
&u_s^1(x, y) = u_s^1(x) e^{-jky \sin\theta}, \quad u_f^1(x, y) = u_f^1(x) e^{-jky \sin\theta} \\
&u_s^2(x, y) = u_s^2(x) e^{-jky \sin\theta}, \quad u_f^2(x, y) = u_f^2(x) e^{-jky \sin\theta}
\end{aligned} \tag{52}$$

Based on the plane motion assumption, Biot's equations reduce to

$$\begin{aligned}
&P \frac{\partial}{\partial x}\left[\frac{\partial u_s^1}{\partial x} + \frac{\partial u_s^2}{\partial y}\right] + N\left(\frac{\partial}{\partial y}\left[\frac{\partial u_s^1}{\partial y} - \frac{\partial u_s^2}{\partial x}\right]\right) + Q \frac{\partial}{\partial x}\left[\frac{\partial u_f^1}{\partial x} + \frac{\partial u_f^2}{\partial y}\right] \\
&\quad = -\omega^2 \tilde{\rho}_{11} u_s^1 - \omega^2 \tilde{\rho}_{12} u_f^1
\end{aligned} \tag{53}$$

$$\begin{aligned}
&P \frac{\partial}{\partial y}\left[\frac{\partial u_s^1}{\partial x} + \frac{\partial u_s^2}{\partial y}\right] - N\left(\frac{\partial}{\partial x}\left[\frac{\partial u_s^1}{\partial y} - \frac{\partial u_s^2}{\partial x}\right]\right) + Q \frac{\partial}{\partial y}\left[\frac{\partial u_f^1}{\partial x} + \frac{\partial u_f^2}{\partial y}\right] \\
&\quad = -\omega^2 \tilde{\rho}_{11} u_s^2 - \omega^2 \tilde{\rho}_{12} u_f^2
\end{aligned} \tag{54}$$

$$R \frac{\partial}{\partial x}\left[\frac{\partial u_f^1}{\partial x} + \frac{\partial u_f^2}{\partial y}\right] + Q \frac{\partial}{\partial x}\left[\frac{\partial u_s^1}{\partial x} + \frac{\partial u_s^2}{\partial y}\right] = -\omega^2 \tilde{\rho}_{12} u_s^1 - \omega^2 \tilde{\rho}_{22} u_f^1 \tag{55}$$

$$R \frac{\partial}{\partial y}\left[\frac{\partial u_f^1}{\partial x} + \frac{\partial u_f^2}{\partial y}\right] + Q \frac{\partial}{\partial y}\left[\frac{\partial u_s^1}{\partial x} + \frac{\partial u_s^2}{\partial y}\right] = -\omega^2 \tilde{\rho}_{12} u_s^2 - \omega^2 \tilde{\rho}_{22} u_f^2 \tag{56}$$

Now new potential functions for plane motion are defined as

$$\begin{aligned}
&\phi_1' = \frac{\partial u_s^1}{\partial x} + \frac{\partial u_s^2}{\partial y}, \quad \phi_2' = \frac{\partial u_s^1}{\partial y} - \frac{\partial u_s^2}{\partial x}, \quad \phi_5' = \frac{\partial u_f^1}{\partial x} + \frac{\partial u_f^2}{\partial y}, \\
&\phi_6' = \frac{\partial u_f^1}{\partial y} - \frac{\partial u_f^2}{\partial x}
\end{aligned} \tag{57}$$

The decoupling procedure for Eqs. (53)–(56) can be applied with the same technique presented in Sec. 2. Now substitution of Eqs. (57) into the resulted equations yields

$$\xi_1 \frac{d^4 \phi_1'}{dx^4} + \xi_4 \frac{d^2 \phi_1'}{dx^2} + \xi_5 \phi_1' = 0 \tag{58}$$

$$N \frac{d^2 \phi_2'}{dx^2} + \left[\omega^2 \left(\tilde{\rho}_{11} - \frac{\tilde{\rho}_{12}^2}{\tilde{\rho}_{22}}\right) - Nk^2 \sin^2\theta\right] \phi_2' = 0 \tag{59}$$

where

$$\begin{aligned}
&\xi_1 = -\frac{Q\lambda_1}{\lambda_3}, \quad \xi_2 = P - \frac{Q\lambda_2}{\lambda_3} - \frac{\omega^2 \tilde{\rho}_{12} \lambda_1}{\lambda_3}, \quad \xi_3 = \omega^2 \left(\tilde{\rho}_{11} - \frac{\tilde{\rho}_{12} \lambda_2}{\lambda_3}\right) \\
&\xi_4 = \xi_2 - 2k^2 \xi_1 \sin^2\theta, \quad \xi_5 = \xi_3 - k^2 \xi_2 \sin^2\theta + k^4 \xi_1 \sin^4\theta
\end{aligned} \tag{60}$$

Equations (58) and (59) are two ordinary differential equations in terms of ϕ_1' and ϕ_2'. The solutions of these equations are obtained as

$$\phi_1'(x) = C_1 e^{\eta_1 x} + C_2 e^{-\eta_1 x} + C_3 e^{\eta_2 x} + C_4 e^{-\eta_2 x} \tag{61}$$

$$\phi_2'(x) = C_5 e^{\eta_3 x} + C_6 e^{-\eta_3 x} \tag{62}$$

where

$$\begin{aligned}
\eta_1 &= \frac{\sqrt{-2\xi_1(\xi_4 + \sqrt{\xi_4^2 - 4\xi_1\xi_5})}}{2\xi_1} \\
\eta_2 &= \frac{\sqrt{2\xi_1(-\xi_4 + \sqrt{\xi_4^2 - 4\xi_1\xi_5})}}{2\xi_1} \\
\eta_3 &= \sqrt{\frac{\omega^2}{N}\left(\tilde{\rho}_{11} - \frac{\tilde{\rho}_{12}^2}{\tilde{\rho}_{22}}\right) - k^2 \sin^2\theta}
\end{aligned} \tag{63}$$

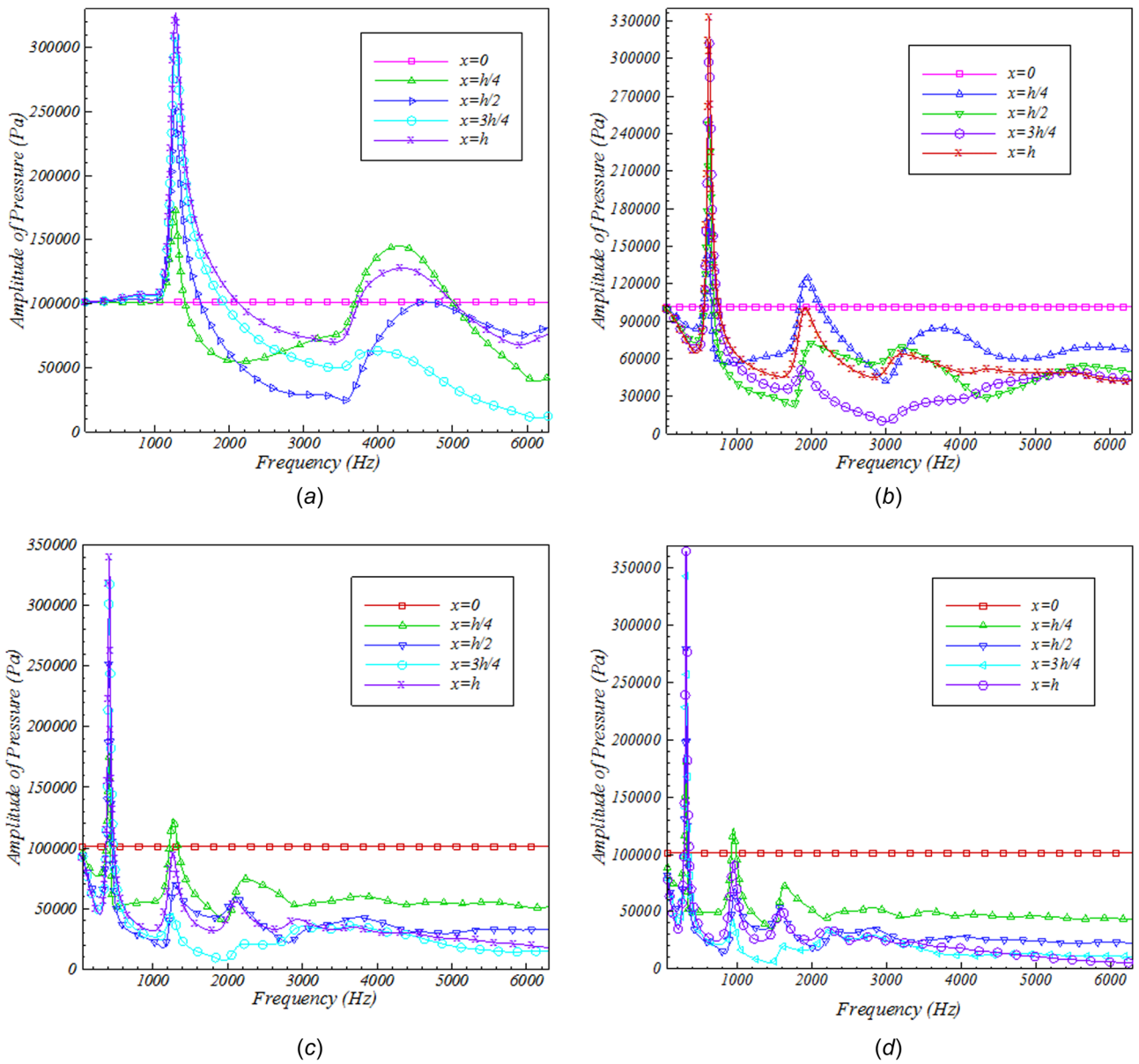

Fig. 6 Variation of amplitude of pressure versus excitation frequency at several locations along the thickness for different foam thicknesses: (*a*) h = 0.05 m, (*b*) h = 0.1 m, (*c*) h = 0.15 m, and (*d*) h = 0.2 m

It should be noted that η_1 and η_2 are the wave numbers for fast and slow compression waves and η_3 expresses the wave number in shear wave defined by Biot [3]. Based on Eqs. (61) and (62), all field variables can be calculated by six unknown parameters C_1 through C_6. Then by satisfying the boundary conditions, unknown parameters can be obtained, explicitly. Consequently, all basic field variables can be determined in terms of frequency and the thickness direction of porous media.

4 Boundary Conditions

Two types of boundary conditions are considered in this section. These boundary conditions can be obtained from the general form presented in Eq. (50).

4.1 Air-Hard Wall Interface. When the layer is a finite thickness and is bonded onto a rigid impervious backing, the boundary conditions yield [21]

$$u_s^1 = 0, \quad u_s^2 = 0, \quad u_f^1 = 0 \tag{64}$$

4.2 Air-Porous Media Interface. Boundary conditions at the surface in contact with air can be written as [21]

$$\sum p = p^e, \quad \sum \sigma_{xx}^t = -p^e, \quad \sum \sigma_{xy}^t = 0 \tag{65}$$

where p^e is the pressure in the free air at contact surface with porous layer. By applying the mentioned boundary conditions, matrix form $[M]\{C\} = \{B\}$ is obtained in which the vector $\{C\}$ are the unknown parameters C_1 through C_6. By solving this matrix equation, six unknown parameters $C_k (k = 1...6)$ are acquired and consequently each field variable can be analytically calculated in all points of the medium.

5 Calculation of Absorption Coefficient

Acoustical parameters, such as the absorption coefficient, can be determined based on potential functions method. The absorption coefficient, α, is defined as [21]

$$\alpha = 1 - |R|^2 \tag{66}$$

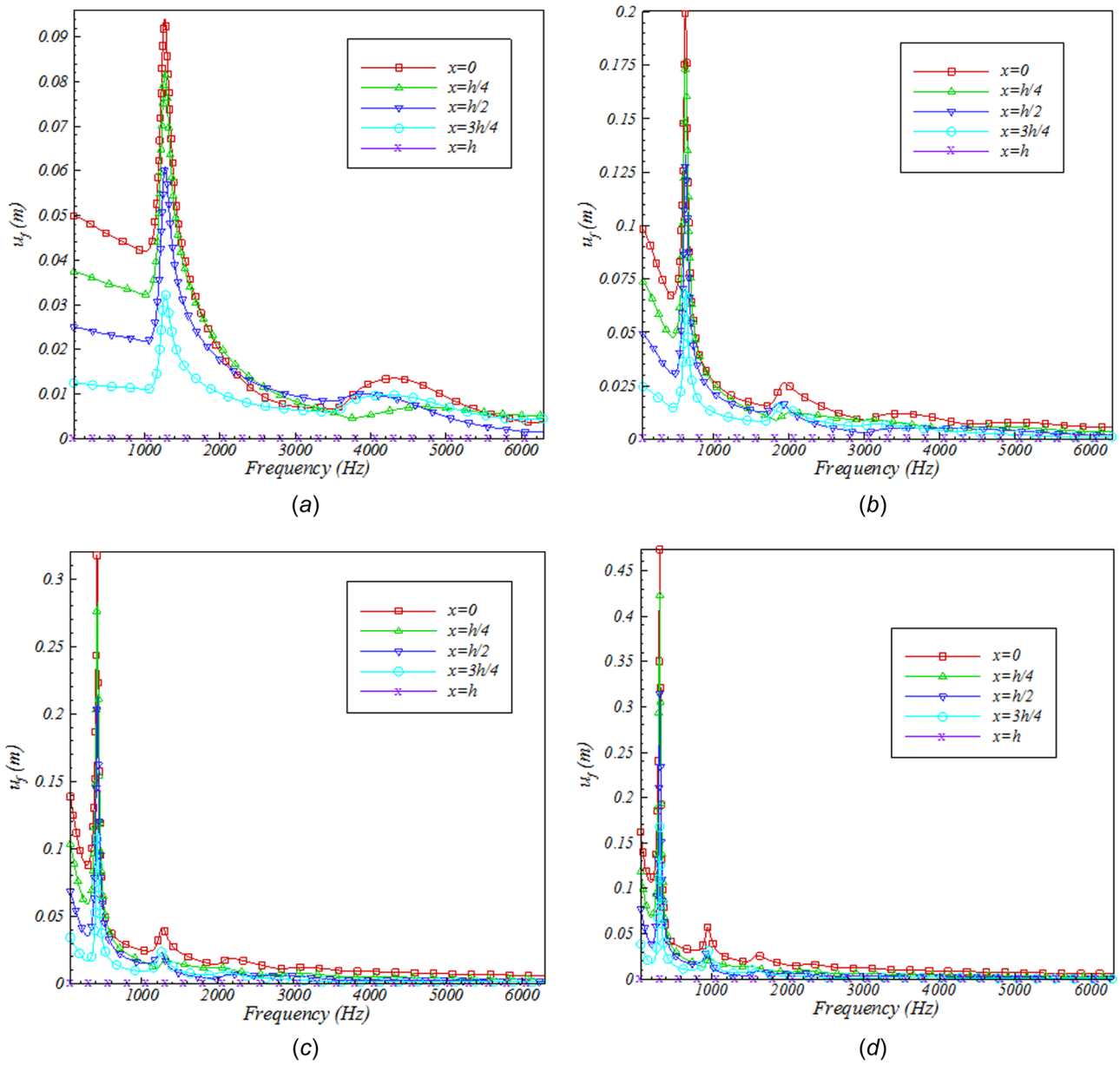

Fig. 7 Variation of amplitude of fluid displacement versus excitation frequency at several locations along the thickness for different foam thicknesses: (*a*) h = 0.05 m, (*b*) h = 0.1 m, (*c*) h = 0.15 m, and (*d*) h = 0.2 m

where R is the reflection coefficient in porous media and is given by

$$R = \frac{(Z - Z_0)}{(Z + Z_0)} \tag{67}$$

In which Z_0 and Z represent the characteristic impedance and the surface impedance in location of $x = 0$, respectively. The surface impedance is defined as $Z = P/V_t$, where P represents pressure and V_t denotes total velocity. It is considered that by satisfying boundary conditions the field variables, P and V_t can be analytically obtained by using potential function method. Then by calculating the surface impedance, the absorption coefficient is determined by using Eqs. (66) and (67).

6 Verification

In this section, for verification of the presented method, the obtained results, e.g., absorption coefficient of the two different foams, have been compared with the corresponding results of the transfer-matrix method. Properties of these foams are shown in Table 1.

Figure 2 shows variation of absorption coefficient of foam 1 versus frequency obtained from both potential function and transfer-matrix methods. This figure indicates very good agreement between the corresponding results. Same comparison for foam 2 has been indicated in Fig. 3. This figure also confirms that the corresponding results of two methods are consistent.

7 Advantages of the New Developed Potential Function Method

The potential function method presented in this paper has some advantages in comparison with the previous methods presented for solving the Biot's equations. The most important advantages of this method are as follows.

In potential function method, by considering general form of Biot's equations and doing some mathematical manipulations, the six-coupled Biot's equations are converted to four-decoupled

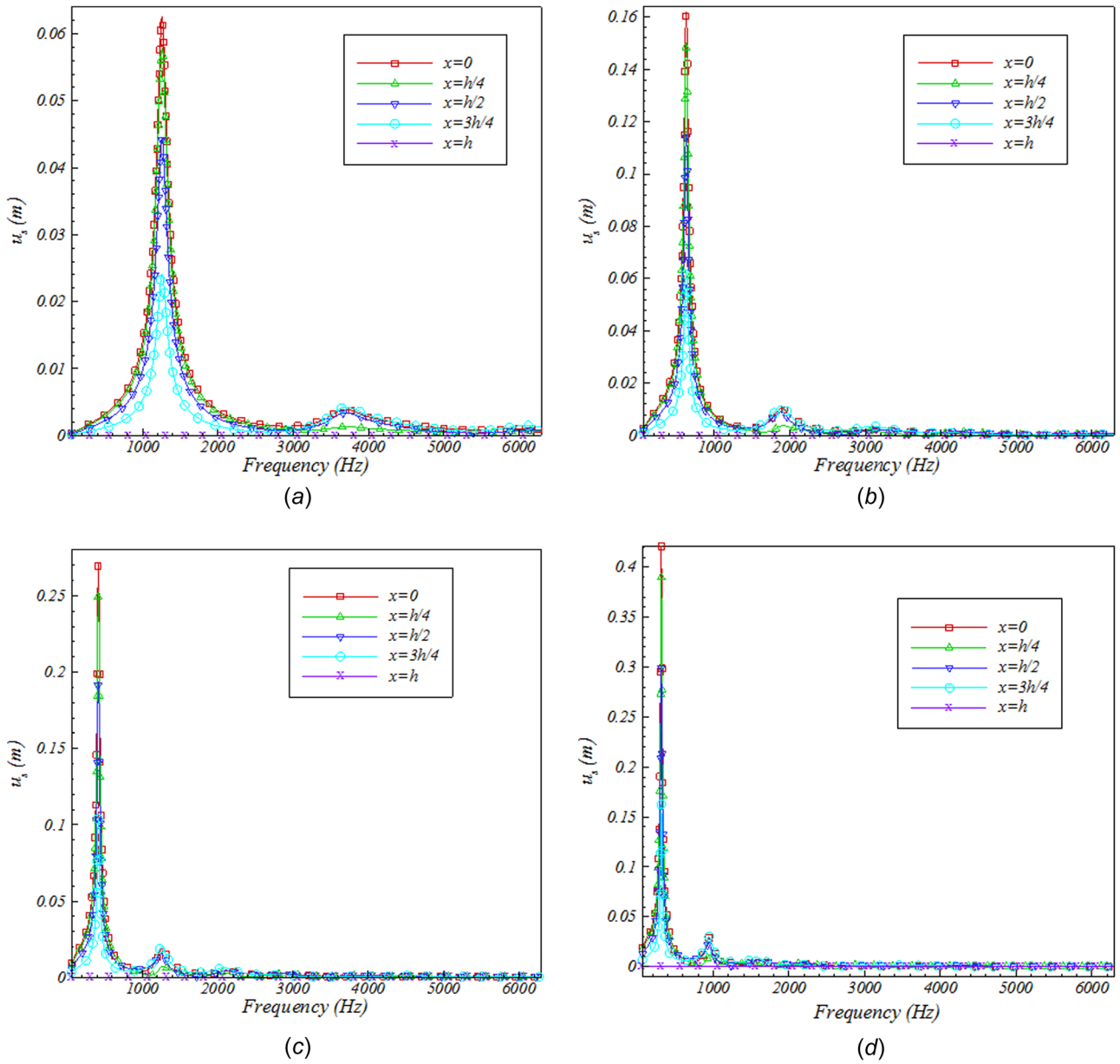

Fig. 8 Variation of amplitude of solid displacement versus excitation frequency at several locations along the thickness for different foam thicknesses: (*a*) h = 0.05 m, (*b*) h = 0.1 m, (*c*) h = 0.15 m, and (*d*) h = 0.2 m

equations in 3D space regardless of any assumption. The decoupled equations can be solved for different boundary conditions and various layers of acoustic materials with analytical method. It is worthwhile to mention that by solving these equations, all field variables of porous material, i.e., pressure and displacement, can be presented analytically, while the previous analytical methods have not been presented these results yet. In other words, the previous analytical methods only calculate parameters such as transmission loss and absorption coefficient and do not provide some other field variables.

Another advantage of this method over the existing methods is that the process of deriving equations in potential function method is based on operators (i.e., $\nabla^2, \nabla^4, \ldots$). Therefore, the resulting equations can easily be generalized to other coordinates such as cylindrical coordinates. Biot's equations in cylindrical coordinates are useful for modeling the impedance tube, which subsequently prevent errors of one-dimensional assumption in rectangular coordinates.

In addition, the results of the potential function method provide the possibility of analyzing the natural frequency and damping of sound absorbing materials. Indeed, by calculating the variations of solid and fluid displacements and pressure of these materials in the frequency domain, damped and undamped natural frequencies and damping coefficients of porous materials can be easily calculated. As a result, these properties are the basic characteristics of porous materials, and effects of each parameter on the mechanical and acoustical properties of porous materials can be studied.

8 Results and Discussion

In this section, for foam 1 (see Table 1), normal incident wave has been considered, and variation of pressure, solid, and fluid displacements with respect to frequency and in the thickness direction are presented by using the potential functions method. Analytical results are presented for four different foam thicknesses (h). Figure 4 shows the variation of amplitude of pressure versus position in thickness direction for different frequencies. Figure 4(*a*) indicates that in low frequency region, the pressure slowly decreases up to 500 Hz, and no pressure increase can be observed in this domain. With increasing frequency, a pressure

Table 2 Comparison of damped and undamped natural frequencies of foam 1 with the corresponding frequencies of Eq. (68)

Thickness (h)	First damped natural frequency	First undamped natural frequency	Undamped natural frequency (Eq. (68))	Second damped natural frequency	Second undamped natural frequency
0.05	1260	1375	1291	3697	4620
0.1	629	642	645	1877	2335
0.15	418	423	430	1248	—
0.2	313	315	322	941	—

increase in the thickness direction is observed. The maximum pressure occurs at a frequency of 633 Hz. The value of pressure at this frequency is three times more than the value of p^e at the point of bounded by rigid walls ($x = h$). For frequencies more than 633 Hz up to 1700 Hz, the pressure reduction is significant (Figs. 4(*a*) and 4(*b*)). Again around 1933 Hz, an increase in pressure can be observed. At this frequency, significant changes in pressure along thickness direction are found. Figures 4(*c*) and 4(*d*) indicate that for frequencies greater than 2500 Hz, the pressure value inside the porous material is less than the exciting pressure, p^e, and pressure fluctuation along the thickness is more severe with increasing frequency. For high frequencies, the material pressure drop with increasing frequency is evident. This phenomenon is attributed to the increase in dissipation of acoustical energy in the porous material as frequency increases. In Fig. 5, variation of absorption coefficient of foam 1 versus exciting frequency is indicated for four different material thicknesses. It can be seen that by increasing material thickness, sound absorption efficiency is improved in the low frequency range smaller than 1000 Hz, as expected.

Figure 6 shows the variation of amplitude of pressure versus excitation frequency for different thicknesses at several locations along the thickness. It can be seen that maximum pressure is found at low frequencies, and for different thicknesses, maximum pressure at various points along the thickness direction always occurs at the same frequency. Similarly, the second maximum of pressure happens at the same frequency for different positions of porous material in the thickness direction, and the loss of pressure for the second peak is noticeable. Furthermore, a closer look to Figs. 5 and 6 indicates that increasing the thickness of the porous material, the maximum amount of pressure is transmitted in the lower frequencies and the acoustic absorption coefficient of the material is improved at lower frequencies. In other words, these figures indicate the relation between sound absorption performance improvement at low frequencies and maximum pressure transmission to the lower frequencies with the increase of material thickness.

Figures 7 and 8 present variation of fluid and solid displacements versus frequency at different locations of thickness direction for different thicknesses. It can be seen that maximum amount of fluid and solid displacements occur at the same frequencies where there is maximum pressure.

Unlike the maximum pressure, the maximum value of fluid and solid displacements increases with increasing thickness. For example, by increasing thickness from 0.05m to 0.2m, the maximum value of solid displacement is increased seven times at the first frequency. As shown in Figs. 6–8, maximum values of amplitude, pressure, and solid and fluid displacements occur at the same frequencies, which correspond with the damped natural frequencies of porous material, as described in Sec. 9. At these frequencies, the maximum pressure happens at the hard wall interface ($x = h$) and pressure increases through thickness direction from the surface in contact with air ($x = 0$) to the surface of hard wall interface ($x = h$). In contrast, maximum fluid and solid displacements decrease from free surface ($x = 0$) to hard wall surface ($x = h$), as expected.

9 Damped and Undamped Natural Frequencies

Natural frequency is the fundamental property of the porous materials, and determination of this frequency is critical and applicable for advancing in mechanical and acoustical research of porous material. By presenting the variation of different field variables versus frequency, via the new developed potential function method, damped natural frequencies of porous media can be determined. These frequencies correspond to the frequencies at which maximum values of field variables occur.

On the other hand, the undamped natural frequency of porous materials is obtained by setting the imaginary part of impedance equal to zero [23]. Also, based on experimental observations, the undamped natural frequency can be obtained as follows [24]:

$$f_r = \frac{1}{4h}\sqrt{\frac{\hat{P} + \gamma p^e}{\rho_s + \phi\rho_f}} \tag{68}$$

where p^e is the pressure in free air and h represents the thickness of porous material. Also, the parameter $\hat{P}$ is defined as

$$\hat{P} = \frac{(1-\nu)E}{(1+\nu)(1-2\nu)} \tag{69}$$

The resonance frequency, f_r, has been observed experimentally. This frequency has been suggested based on the peak of variations in real and imaginary parts of the surface impedance. Also, frequency of f_r is related to longitudinal plane waves propagating in the direction normal to the surface. Therefore, vibrational mode corresponding to this frequency represents axial deformation. It is noteworthy that Eq. (68) has been obtained based on the simple rigid frame model, with the assumption that the interaction between air and the frame is negligible [25].

In this paper, first two damped natural frequencies are obtained using Figs. 6–8, and undamped natural frequencies are calculated by setting the imaginary part of the impedance equal to zero. Finally, in Table 2, the obtained results for different thicknesses are compared with the corresponding results of Eq. (68).

As expected, the results presented for damped natural frequencies are less than the corresponding undamped natural frequencies and by increasing thickness, natural frequency decreases. Table 2 indicates that the effect of damping on the first natural frequency is reduced for higher values of foam thickness and for lower values of thickness (i.e., $h = 0.05$m), damping the first natural frequency up to 8.5%. However, damping effects increase for the second natural frequency up to 25%.

In addition, Table 2 shows the acceptable agreement (less than 5% difference) between the first natural frequency obtained from the potential function method and the corresponding results of experimental relation (68) presented in Ref. [24].

Figure 9 shows variation of amplitude of pressure versus position in thickness direction and excitation frequency in 3D diagram. It can be seen that for each value of thickness, the maximum amplitude of pressure occurs in the damped natural frequency at the position of hard wall interface ($x = h$). Therefore, by exciting the porous material with its damped natural frequency, maximum amount of pressure in the media can be obtained. This note is important for different applications of industry. For example, in the process of extracting oil from the soil, maximum displacement and pressure can be obtained in different position of thickness direction when the soil is excited by the specific frequency.

10 Conclusions

In this paper, a new exact solution for solving the Biot's equations has been presented based on potential function method. The primary coupled Biot's equations based on fluid and solid displacements in 3D space have been considered. By defining some potential functions and doing some mathematical manipulations, the six-coupled Biot's equations have been converted to four-decoupled equations in 3D space without any assumption. Then, by considering the incident plane waves and applying boundary conditions, the partial differential equations have been converted to ordinary differential equations and have been analytically solved. For verification of the presented method, absorption coefficient of the two different foams have been compared with the corresponding results of the transfer-matrix

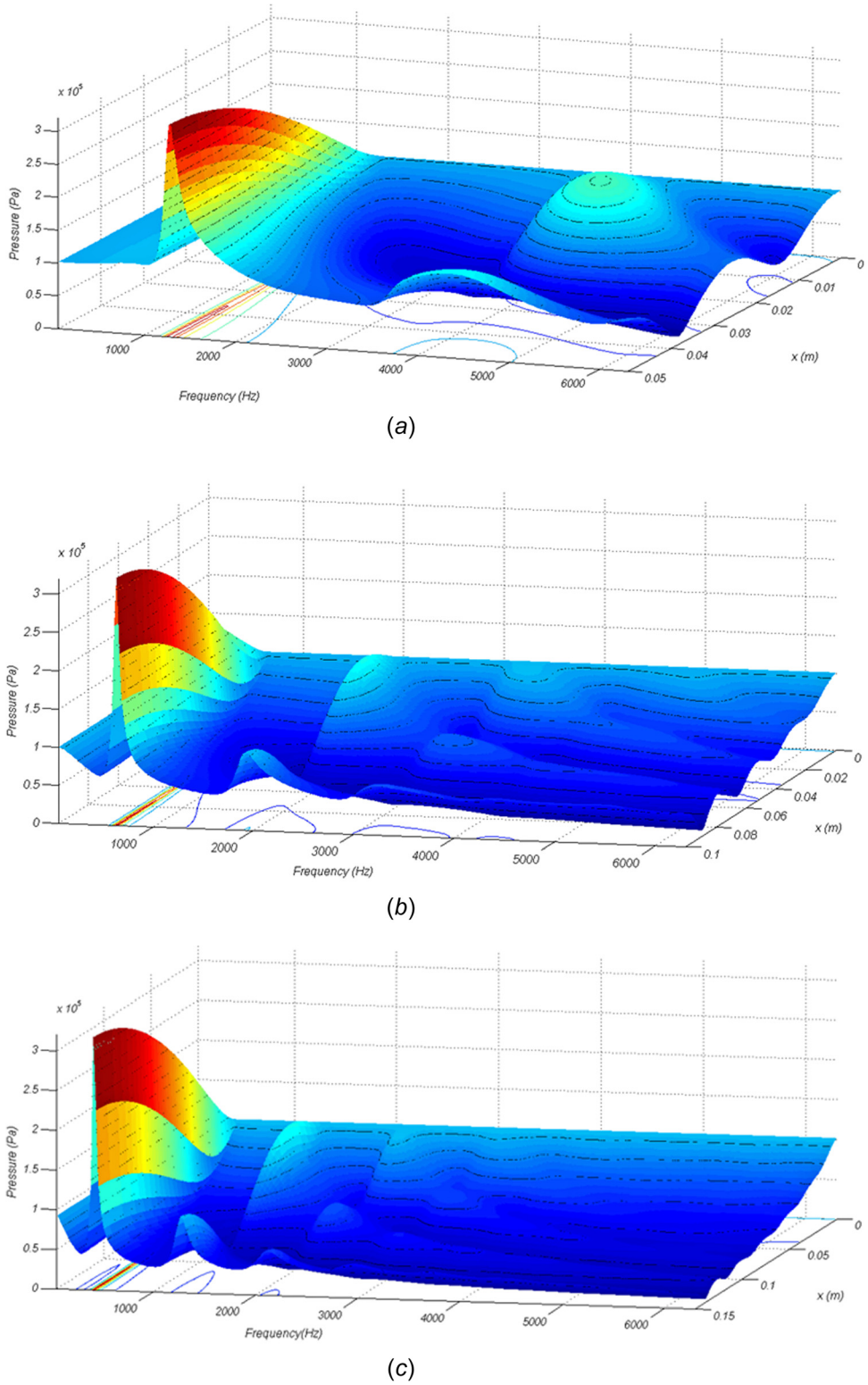

Fig. 9 3D representation for variation of pressure amplitude versus frequency and position in thickness direction for three different foam thicknesses: (*a*) h = 0.05 m, (*b*) h = 0.1 m, and (*c*) h = 0.15 m

method. In conclusion, after describing some advantages of the new developed potential function method over previous analytical methods, variation of field variables, i.e., pressure and solid and fluid displacements versus frequency and position in the thickness direction have been presented. Finally, damped and undamped natural frequencies of porous media have been obtained, and comparison has been done with the corresponding results of experimental base formulation. The following conclusions are remarked:

(1) Variation of absorption coefficient versus frequency due to the new developed potential function method is in very good agreement with the corresponding results of transfer-matrix method.
(2) With the use of the new developed solution, all field variables of porous media can be determined. Consequently, fundamental features, such as damped and undamped natural frequencies, and damping coefficient of porous materials are calculated using the variations of field variables versus frequency.
(3) Maximum values of pressure and fluid and solid displacements happen at the same frequencies named damped natural frequencies.
(4) The value of pressure inside the material at the rigid wall boundary is three times more than the exciting pressure, p^e, when the media is excited with its first damped natural frequency.
(5) Unlike the maximum pressure, by increasing thickness, the maximum value of solid and fluid displacements increases.
(6) With increasing the thickness of porous material, the maximum amount of pressure is transmitted to the lower frequencies and the acoustic absorption coefficient of the material is improved at lower frequencies.
(7) Damping decreases the first natural frequency of the foam up to 8.5%, where as its effect is much more for the second natural frequency.
(8) First undamped natural frequencies obtained from the potential function method are in good agreement (less than 5% difference) with the corresponding results for experimental relation presented in Ref. [24].
(9) By increasing material thickness, the effect of damping on the first damped natural frequency of porous media decreases.

References

[1] Attenborough, K., 1982, "Acoustical Characteristics of Porous Materials," Phys. Rep., **82**(3), pp. 179–227.
[2] Schanz, M., 2009, "Poroelastodynamics: Linear Models, Analytical Solutions, and Numerical Methods," ASME Appl. Mech. Rev., **62**(3), p. 030803.
[3] Biot, M. A., 1956, "Theory of Propagation of Elastic Waves in a Fluid-Saturated Porous Solid. I. Low-Frequency Range," J. Acoust. Soc. Am., **28**(2), pp. 168–178.
[4] Biot, M. A., 1956, "Theory of Propagation of Elastic Waves in a Fluid-Saturated Porous Solid. II. Higher-Frequency Range," J. Acoust. Soc. Am., **28**(2), pp. 179–191.
[5] Dai, Z., Peng, Y., Mansy, H. A., Sandler, R. H., and Royston, T. J., 2014, "Comparison of Poroviscoelastic Models for Sound and Vibration in the Lungs," ASME J. Vib. Acoust., **136**(5), p. 051012.
[6] Atalla, N., Panneton, R., and Debergue, P., 1998, "A Mixed Displacement-Pressure Formulation for Poroelastic Materials," J. Acoust. Soc. Am., **104**(3), pp. 1444–1452.
[7] Dazel, O., Brouard, B., Depollier, C., and Griffiths, S., 2007, "An Alternative Biot's Displacement Formulation for Porous Materials," J. Acoust. Soc. Am., **121**(6), pp. 3509–3516.
[8] Burridge, R., and Vargas, C., 1979, "The Fundamental Solution in Dynamic Poroelasticity," Geophys. J. Int., **58**(1), pp. 61–90.
[9] Moore, J. A., and Lyon, R. H., 1982, "Resonant Porous Material Absorbers," J. Acoust. Soc. Am., **72**(6), pp. 1989–1999.
[10] Chin, R., Berryman, J., and Hedstrom, G., 1985, "Generalized Ray Expansion for Pulse Propagation and Attenuation in Fluid-Saturated Porous Media," Wave Motion, **7**(1), pp. 43–65.
[11] Allard, J. F., Bourdier, R., and Depollier, C., 1986, "Biot Waves in Layered Media," J. Appl. Phys., **60**(6), pp. 1926–1929.
[12] Allard, J. F., Depollier, C., Rebillard, P., Lauriks, W., and Cops, A., 1989, "Inhomogeneous Biot Waves in Layered Media," J. Appl. Phys., **66**(6), pp. 2278–2284.
[13] Bolton, J. S., Shiau, N. M., and Kang, Y., 1996, "Sound Transmission Through Multi-Panel Structures Lined With Elastic Porous Materials," J. Sound Vib., **191**(3), pp. 317–347.
[14] Kang, Y. J., and Bolton, J. S., 1995, "Finite Element Modeling of Isotropic Elastic Porous Materials Coupled With Acoustical Finite Elements," J. Acoust. Soc. Am., **98**(1), pp. 635–643.
[15] Goransson, P., 1998, "A 3-D, Symmetric, Finite Element Formulation of the Biot Equations With Application to Acoustic Wave Propagation Through an Elastic Porous Medium," Int. J. Numer. Methods Eng., **41**(1), pp. 167–192.
[16] Goransson, P., 1995, "Acoustic Finite Element Formulation of a Flexible Porous Material—A Correction For Inertial Effects," J. Sound Vib., **185**(4), pp. 559–580.
[17] Tanneau, O., Lamary, P., and Chevalier, Y., 2006, "A Boundary Element Method for Porous Media," J. Acoust. Soc. Am., **120**(3), pp. 1239–1251.
[18] Biot, M. A., and Willis, D. G., 1957, "The Elastic Coefficients of the Theory of Consolidation," ASME J. Appl. Mech., **24**(4), pp. 594–601.
[19] Johnson, D. L., Koplik, J., and Dashen, R., 1987, "Theory of Dynamic Permeability and Tortuosity in Fluid-Saturated Porous Media," J. Fluid Mech., **176**(1), pp. 379–402.
[20] Champoux, Y., and Allard, J. F., 1991, "Dynamic Tortuosity and Bulk Modulus in Air-Saturated Porous Media," J. Appl. Phys., **70**(4), pp. 1975–1979.
[21] Allard, J. F., and Atalla, N., 2009, *Propagation of Sound in Porous Media: Modelling Sound Absorbing Materials*, 2nd ed., Wiley, Chichester, UK.
[22] Atalla, N., Sgard, F., and Amedin, C. K., 2006, "On the Modeling of Sound Radiation From Poroelastic Materials," J. Acoust. Soc. Am., **120**(4), pp. 1990–1995.
[23] Kinsler, L. E., Frey, A. R., Coppens, A. B., and Sanders, J. V., 1999, *Fundamentals of Acoustics*, 4th ed., Wiley, New York.
[24] Allard, J. F., Depollier, C., Guignouard, P., and Rebillard, P., 1991, "Effect of a Resonance of the Frame on the Surface Impedance of Glass Wool of High Density and Stiffness," J. Acoust. Soc. Am., **89**(3), pp. 999–1001.
[25] Bardot, A., Brouard, B., and Allard, J. F., 1996, "Frame Decoupling at Low Frequency in Thin Porous Layers Saturated by Air," J. Appl. Phys., **79**(11), pp. 8223–8229.